

Strong influence of non-ideality of electrodes on stability of single domain state in ferroelectric-paraelectric superlattices

A. P. Levanyuk and I. B. Misirlioglu

Citation: [Journal of Applied Physics](#) **119**, 024109 (2016); doi: 10.1063/1.4939779

View online: <http://dx.doi.org/10.1063/1.4939779>

View Table of Contents: <http://scitation.aip.org/content/aip/journal/jap/119/2?ver=pdfcov>

Published by the [AIP Publishing](#)

Articles you may be interested in

[Ferroelectric properties of BaZrO₃/PbZrO₃ and SrZrO₃/PbZrO₃ superlattices: An ab-initio study](#)

[J. Appl. Phys.](#) **116**, 074112 (2014); 10.1063/1.4893300

[Phase transitions in ferroelectric-paraelectric superlattices: Stability of single domain state](#)

[Appl. Phys. Lett.](#) **103**, 192906 (2013); 10.1063/1.4829149

[Direct determination of the effect of strain on domain morphology in ferroelectric superlattices with scanning probe microscopy](#)

[J. Appl. Phys.](#) **112**, 052011 (2012); 10.1063/1.4746081

[Phase transitions in ferroelectric-paraelectric superlattices](#)

[J. Appl. Phys.](#) **110**, 114109 (2011); 10.1063/1.3662197

[High dielectric tunability in ferroelectric-paraelectric bilayers and multilayer superlattices](#)

[Appl. Phys. Lett.](#) **88**, 132904 (2006); 10.1063/1.2189909



NEW Special Topic Sections

NOW ONLINE
Lithium Niobate Properties and Applications:
Reviews of Emerging Trends

AIP | Applied Physics Reviews

Strong influence of non-ideality of electrodes on stability of single domain state in ferroelectric-paraelectric superlattices

A. P. Levanyuk^{1,2} and I. B. Misirlioglu³

¹*Department of Physics, University of Washington, Seattle, Washington 98105, USA*

²*Moscow State Technical University of Radioengineering, Electronics and Automation (MSTU-MIREA), Moscow 119454, Russia*

³*Faculty of Engineering and Natural Sciences, Sabanci University, Tuzla/Orhanli 34956, Istanbul, Turkey*

(Received 18 August 2015; accepted 30 December 2015; published online 13 January 2016)

We study the phase stabilities with respect to small perturbations in ferroelectric-paraelectric superlattices and show that nature of the electrodes characterized by a deviation from the ideal behavior strongly influences the possibility to obtain single-domain state in ferroelectric-paraelectric superlattices. To demonstrate this, we analyze the limit of stability of the paraelectric and the single domain state in ferroelectric-paraelectric superlattices in contact with top and bottom electrodes with finite screening lengths. The combined analytical and numerical analyses of one bilayer and two bilayer systems are carried out using the Landau-Ginzburg-Devonshire formalism and equations of electrostatics. The BaTiO₃/SrTiO₃ system was considered as an example. Unlike the case of ideal electrodes where the stability limits are independent of the system size, the stability analysis in a multilayer with real electrodes should take into account explicitly the number of the repeating units that makes the algebra very cumbersome, forcing us to consider systems with one and two bilayer stacks only. Extrapolating the difference between the two systems to the cases of many repeating units gives us the possibility to make qualitative but feasible predictions related to those with many repeating units. We observe that in systems with nearly equal thicknesses of the ferroelectric and paraelectric layers, the electrodes with realistic screening lengths lead to dramatic widening of the parametric region where the single-domain state is absolutely unstable expelling the single-domain state to unphysical layer thicknesses and temperatures. This region grows when one goes from a single bilayer to two bilayer system, implying that obtaining a single domain state becomes even less feasible in systems with many bilayers. When electrode properties approach that of ideal in addition to increasing the volume fraction of the ferroelectric component, the effect of growth of the region of absolute instability of the single domain state may remain very strong for relatively thin repeating units (a few nanometers). This tendency will continue with increasing the number of the repeating units. © 2016 AIP Publishing LLC. [<http://dx.doi.org/10.1063/1.4939779>]

I. INTRODUCTION

Ferroelectric-paraelectric (FE-PE) multilayers or superlattices are on the agenda of research groups in the search of generating new functionalities via the idea of exposing constituent layers to one another in a periodic manner. Quite a number of systematic experimental and theoretical works are devoted to revealing their interesting properties since early 90s.^{1–27} Despite this effort, it can be stated that the theoretical understanding of properties of these systems is at an initial state and its progress presents many more challenges than previously anticipated. In this paper, we mean by multilayers periodic structures with ferroelectric layers having one polar axis perpendicular to the layer plane as it is the case in BaTiO₃ (PbTiO₃)/SrTiO₃ stacks coherently grown on SrTiO₃ substrates. In such systems consisting of FE layers contacting PE ones, single domain ferroelectric states imply existence of the depolarizing fields because of interfaces between the layers. A straight consequence of these fields is a tendency to form a ferroelectric domain structure in the superlattices whose theoretical study has been initiated in Ref. 6 by the method employed earlier in the work of Chensky and Tarasenko²⁸ (for a recent review see Ref. 29)

to address a similar problem for a ferroelectric plate with dielectric “dead layer” between the plate and the short-circuited electrodes. Qualitatively, the obtained results were similar to those of Ref. 28 which is not surprising since the periodic boundary conditions assumed in Ref. 6 were equivalent to the short-circuited conditions of Ref. 28. Specifically, it was found for superlattices with equal thicknesses of ferroelectric and paraelectric layers that, for small thicknesses, the phase transition from the paraelectric phase is into single-domain (SD) state, while for larger thicknesses it is into a multi-domain (MD) state. Though the assumption about periodical boundary conditions was later found invalid for multidomain states in almost any multilayer of the considered type,¹⁶ the qualitative character of the phase diagram for SD and MD states remains the same. Based on the results of Refs. 28 and 29, it could be expected that upon further cooling after PE-MD phase transition, the stability of the SD state with respect to small perturbations would be recovered though this recovery would lead to a metastable state. This means that, in the ferroelectric layer thickness-temperature ($l - T$) diagram, there exists a region between two curves of stability loss of PE and SD states with the upper curve being the PE-to-MD transition and the lower curve is the

overheating limit of the SD state above which the SD state is absolutely unstable. At sufficiently low thicknesses, these curves merge where the transition from the PE state is into SD state (see Ref. 23).

The above-mentioned theoretical result has been obtained by assuming the electrodes of the multilayer as ideal, i.e., the electric fields cannot penetrate into the electrode and the bound polarization charges are screened right at the superlattice/electrode interface. This might seem a non-important assumption but our results in Ref. 16 obtained by the same method as that of Refs. 28, 29, and 6 revealed the extreme sensitivity of the ferroelectric phase transition to specific features of the near electrode region of superlattices with ideal electrodes. Implicitly, this meant that the character of the electrodes, in particular, a finite penetration length of the electric field (usually less than 1 Å for metals), may be expected to strongly impact the properties of multilayers. Both this observation and experimental evidence of strong dependence of properties of superlattices on the character of the electrodes¹⁵ motivated us to carry out the present study. We use once again the same method as in Refs. 6, 28, 29, and 16 but abandon the assumption about ideal electrodes so that the electric field is now allowed to penetrate into the electrode a finite distance that we model as a thin dielectric layer (see Ref. 29 for a detailed treatment of the topic). We encounter the same difficulty as any theoretical studies of the multilayers of the considered type: as we have shown earlier,¹⁶ when treating MD states, a seemingly natural assumption that considers the spatial distribution of ferroelectric polarization appearing at the phase transition being periodic along the superstructure is almost always incorrect even in the case of ideal electrodes. There is no reason to expect it to be correct even in some special case if the electrodes are non-ideal. That is why we were forced to restrict ourselves by two simple systems with non-ideal electrodes: one or two units of FE-PE bilayers. The analytical calculations imply, even for these systems, a fairly tedious algebra and cannot be reasonably finished and presented without extensive numerical efforts.

We explicitly show that the quality of the electrodes has a dramatic influence on the region of absolute instability of SD state, which becomes larger with respect to the case of ideal electrodes. The increase is larger for 2 bilayers (2BL) than for 1BL implying increasing of this region with increasing number of units for a system with non-ideal electrodes. The difference is both due to shift down of the curve of stability of SD state and shift up of the curve of stability loss of PE phase. If this tendency continues for systems with more bilayers, this region where only MD phase is possible is the narrowest for 1BL comparing with the systems with the same non-ideal electrodes and larger number of the BL. We would like to emphasize that for BaTiO₃/SrTiO₃ systems, which we take as a model system, we find no room for SD state for equal thickness of the layers at physically meaningful temperatures and layer thicknesses for realistic parameters of the electrode even in the case of 1 BL. It is expected to be even more so for larger number of the BL units given the above mentioned tendency. For systems where the FE layer is considerably thicker than the PE one, the stability

limit of the SD state, in the presence of real electrodes, can be above room temperature in multilayers considered here. The limit of SD stability region of the 2 BL system, however, corresponds to relatively lower temperatures than the 1 BL one, allowing us to conclude that the SD stability for systems with many units will be less feasible. This qualitative outcome is the same as that of the case where FE and PE layers have equal thickness.

We address the problem within the same continuous medium approach that was used in several previous works. Basically, we study the limits of stability of the PE phase and the SD state of the ferroelectric phase. The method can be traced back to the book³⁰ where it was used to find critical fields of type-II superconductors within the Ginzburg-Landau theory. It was later applied to ferroelectrics by Chensky and Tarasenko²⁸ followed by several other authors (see, e.g., Refs. 6, 16, 23, and 26). The non-ideality of the electrodes we model by a very thin “dead layer” at the electrode surface. This is almost equivalent to introducing the Thomas-Fermi screening length to take into account partial penetration of electric field into the metal, see Ref. 29. We have taken into account only electrostatic effects of interfaces between the layers and between the material and the electrodes because of the above mentioned difficulties in the calculations.

The paper is organized as follows: In Sec. II, the method used is shortly outlined. In Sec. III, we find the limits of stability of the paraelectric phase, i.e., temperature of paraelectric-ferroelectric phase transition. We carry out the calculations for 1BL system with real electrodes and only report the results for 2BL ones that are obtained by the very same method as for 1BL but with a much more involved algebra due to the presence of more interfaces at which boundary conditions apply. In Sec. IV, we find the limits of stability of SD state. This limit is not a SD to MD transition. This transition, which we do not find, is discontinuous²⁹ and what we find in this study corresponds to the limit of superheating of the SD state, i.e., its existence during application wise desirable time can be realized (if possible at all) only below the calculated temperatures of the stability loss. In Sec. V, we compare and comment on the FE layer thickness-temperature ($l - T$) phase diagrams for different electrodes and for two values of thickness ratios of the layers. In Sec. VI, we summarize the results of the paper emphasizing simplifications made when obtaining these results.

II. METHOD

We consider the BaTiO₃/SrTiO₃ system strained on a thick SrTiO₃ substrate (see Figure 1 for the schematics). Using the notations of Ref. 23, the properties of the ferroelectric are described by the equation of state within the Landau-Ginzburg-Devonshire (LGD) theory

$$AP_z + BP_z^3 - g \frac{\partial^2 P_z}{\partial x^2} - g \frac{\partial^2 P_z}{\partial y^2} - \eta \frac{\partial^2 P_z}{\partial z^2} = E_z, \quad (1)$$

where the gradient terms are in accordance with the tetragonal symmetry of the paraelectric phase. Here, P_z is

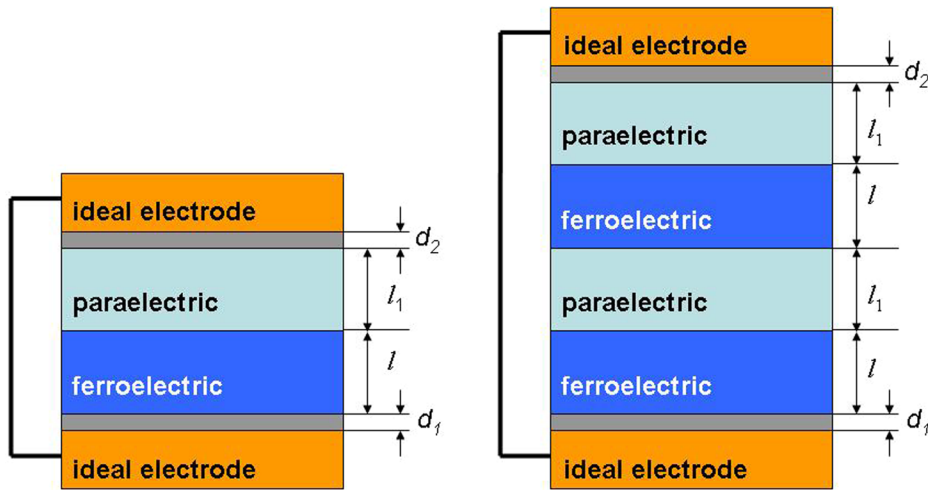


FIG. 1. Schematics of the 1 BL and 2 BL stacks analyzed in this work.

ferroelectric polarization normal to the plane of the stack, g and η are the coefficients of gradient energy, and E_z is the electric field. A in Eq. (1) is the “misfit modified”³¹ coefficient containing the temperature dependence given as $A = (T - \hat{T}_C)/(\epsilon_0 C) + u_m[Q_{12}^2/(S_{11} + S_{12})] = (T - T_C)/(\epsilon_0 C)$ with \hat{T}_C being the transition temperature of the stress free crystal in the absence of depolarizing fields, ϵ_0 is the permittivity of vacuum in International System of Units (SI), C is the Curie constant, u_m is the misfit strain, and Q_{12} , S_{11} , and S_{12} are electrostrictive and elastic compliance constants of the FE crystal. The coefficient B is positive since according to Ref. 31 the first order PE-FE phase transition in BaTiO₃ becomes a second order one because of partial clamping by the substrate. Note that A is modified by the misfit term and therefore the transition temperature will be shifted from \hat{T}_C to T_C , where we denote the latter as the transition temperature of the strained film in the absence of depolarizing fields. For a film of BaTiO₃ grown on SrTiO₃, this shift is almost to 600 °C as also documented by several previous works in addition to experimental studies reporting transition temperatures as high as 500 °C.³² The difference is not surprising because, in particular, one has to expect a strong contribution to this transition temperature from the depolarizing fields.

As it is explained in Refs. 28 and 29, it is reasonable for thicknesses of the ferroelectric material larger than that of the atomic lengths to restrict ourselves to a simpler form of Eq. (1) as

$$AP_z + BP_z^3 - g \frac{\partial^2 P_z}{\partial x^2} - g \frac{\partial^2 P_z}{\partial y^2} = E_z. \quad (2)$$

One also needs to take into account the (indirect) influence of P_z on other degrees of freedom. The most important of them is the polarization along x, y (nonferroelectric) axes. Since $E_z(x, y)$ implies the presence of E_x and E_y via the electrostatic equation $\text{curl} \mathbf{E} = 0$, one has to consider this field together with the polarization components P_x, P_y which we shall implicitly take into account by introducing the dielectric constant ϵ_{\perp} along the plane of the structure. The electric field in the paraelectric with the dielectric constant ϵ_p also exists due to the ferroelectric polarization in the FE layer, as well as in the two dead layers with the dielectric constants ϵ_{e1} and ϵ_{e2} . The system of equations become complete by adding $\text{div} \mathbf{D} = 0$,

where $\mathbf{D} = \epsilon_0 \epsilon_{p,e1,e2} \mathbf{E}$ in the paraelectric or the dead layers and $\mathbf{D} = (\epsilon_0 \epsilon_{\perp} E_x, 0, \epsilon_0 \epsilon_b E_z + P_z)$ in the ferroelectric one. In the latter formula, we have introduced the so-called “base” dielectric constant, ϵ_b , which is assumed to model the non-ferroelectric polarization along z -axis apart from P_z which designates here not the total z -component of the polarization but only its “soft part” corresponding to the order parameter.³³

To find the condition of loss of stability of a state with respect to small perturbations, one has to linearize Eq. (2) near the value of P_z in a given state, i.e., near $P_z = 0$ for the PE phase or, for the SD state, near the spontaneous polarization, P_{zS} . The former will be used to find the temperature of the PE-MD state transition and the latter to find the limit of stability of the SD state. One has to study the existence of solutions of the obtained system of linear differential equations subject to the relevant boundary conditions in both cases. A phase (state) is stable with respect to small perturbations when the only possible solution is zero (trivial). Appearance of non-zero (non-trivial) solutions signals the way of loss of stability of the considered phase (state), and specifically this loss is with respect to a form of the ferroelectric polarization distribution which is represented by the solution (see Ref. 29). Within this formulation of the problem, there is infinite number of ways of the stability loss represented by infinite set of polarization distributions. Of course, they are not real; they are virtual possibilities of the stability loss. The real loss of stability of the paraelectric phase occurs with respect to a single form of the polarization distribution among this infinite number of possible solutions and corresponds to the maximum value of A when studying stability of the PE phase and to the minimum value of A when studying stability of the SD ferroelectric state. The criterion of the aforementioned choice is that the loss of stability with respect to this solution occurs the earliest when moving from the state of stability, which occurs either when cooling down from the PE phase or when heating up from the SD state, i.e., it corresponds to the highest temperature in the case of PE phase and to the lowest one in the case of SD ferroelectric state.

Our choice of the system for consideration is worth commenting on also. Apart from a great experimental interest, we found the BaTiO₃/SrTiO₃ system simpler than others, in particular, PbTiO₃/SrTiO₃. This is important because the

effects of the electrodes proved to be very dramatic from one side but very difficult to treat from the other. So that it is worthwhile to demonstrate electrode effects just for the simplest case. We consider our results mainly as qualitative given that it proved unfeasible to obtain numerical results for systems with more than two bilayers even when taking into account electrostatic effects only. In view of this, it seems reasonable to simplify the problem for the BaTiO₃/SrTiO₃ system as well. Specifically, we neglect temperature dependence of the dielectric constant for the directions perpendicular to the polar axis (ε_{\perp}). This quantity is known, since long ago, to be important for the domain structure formation (see, e.g., Refs. 16, 28, and 29). In bulk uniaxial ferroelectrics, this quantity can be usually considered as temperature-independent. This is not, however, the case when the uniaxiality (tetragonality) is due to misfit strain imposed on a material which is cubic in the paraelectric phase. For BaTiO₃/SrTiO₃ system, the value of ε_{\perp} in the paraelectric phase of BaTiO₃ changes from about 100 at $T = 600^{\circ}\text{C}$ to about 350 at -273°C . When studying stability of this phase, we use an intermediate value of 250. Note that such a simplification would be impossible for the PbTiO₃/SrTiO₃ system where ε_{\perp} of the paraelectric phase becomes infinite at $T = 123^{\circ}\text{C}$ so that temperature dependence of ε_{\perp} should be explicitly taken into account when treating domain formation in this system. In SD state, the value of ε_{\perp} is influenced by the value of spontaneous polarization. Taking into account that, for the cases considered in this work, the SD state never exists at temperatures higher than 200°C (for realistic parameters of the electrodes as we demonstrate), we find that ε_{\perp} changes from 100 to about 350 in this state. We fix this value once more as 250 when studying stability of this state. Note that choosing of the minimum or maximum values of ε_{\perp} of SD state does not change significantly the results. The dielectric constant of SrTiO₃ is also taken as temperature-independent and equal to 300 which corresponds to the room temperature value. At $T = -200^{\circ}\text{C}$, this constant is already about 1000 and becomes much higher close to 0 K. This underlines once again that our results for low temperatures should be considered rather as illustrative than definite.

III. LIMIT OF STABILITY OF PARAELECTRIC PHASE

To simplify the problem, we consider that the ferroelectric is isotropic in the x - y plane and paraelectric is also isotropic in all directions. Then, the nontrivial inhomogeneous solutions appear simultaneously along all the directions in the x - y plane. Therefore, it is sufficient to consider polarization distributions along one direction only, which we identify as the x -axis. According to the statement of the method in Section II, one can express the linearized constituent equation for the ferroelectric polarization, P_z , as

$$AP_z - g \frac{\partial^2 P_z}{\partial x^2} = E_z. \quad (3)$$

Since we are considering slabs infinite along the plane, we can present the x -dependence of all the functions in form of a Fourier series, e.g., $P_z(x, z) = \sum P_{zk}(z) \cos kx$, and the electrical potential φ , from which the electric field E_z is calculated,

can be expressed as $\varphi(x, z) = \sum \varphi_k(z) \sin kx$ to see that the system of the partial differential equations decomposes into ordinary differential equations. It is convenient to use the electrical potential $\varphi(x, z)$ instead of the electric field. Inserting the Fourier form of the polarization and the electrostatic potential, Eq. (3) converts into an algebraic equation

$$(A + gk^2)P_{zk} = -\frac{d\varphi_k}{dz}, \quad (4)$$

and for a given k the system of our equations then acquires the form

$$\varepsilon_k \frac{d^2 \varphi_{fk}}{dz^2} - \varepsilon_{\perp} k^2 \varphi_{fk} = 0, \quad (5)$$

where

$$\varepsilon_k = \varepsilon_b + 1/\varepsilon_0(A + gk^2), \quad (6)$$

for the ferroelectric. For the paraelectric layer and the dead layers, we have the Laplace equation expressed in terms of the Fourier components

$$\frac{d^2 \varphi_{p,dk}}{dz^2} - k^2 \varphi_{p,dk} = 0. \quad (7)$$

The boundary conditions at interfaces between two dielectrics are the standard electrostatic ones: continuity at the interface of the potential and of the component of \mathbf{D} normal to the plane. We are considering short-circuited system putting the potential to zero at surface of the ideal metal electrodes which represent the bulk of the real metallic electrodes in our case since the surfaces of the electrodes are considered to have dead layers (behaving like a dielectric where the electric field can penetrate). The loss of stability occurs when $\varepsilon_k < 0$ only^{28,29} and in this case the general solution of Eq. (5) is a linear combination of $\sin qz$ and $\cos qz$, where

$$q = k\sqrt{\varepsilon_{\perp}/|\varepsilon_k|}, \quad (8)$$

while the general solution of Eq. (7) is a linear combination of $\sinh kz$ and $\cosh kz$.

Now we shall consider one bilayer with two real electrodes, i.e., we have a system consisting of an ideal metal ($z < 0$), the first “dead layer,” i.e., a linear dielectric with $\varepsilon = \varepsilon_{e1}$ ($0 < z < d_1$), the ferroelectric ($d_1 < z < l + d_1$), the paraelectric ($l + d_1 < z < l + l_1 + d_1$), the second “dead layer,” i.e., again a linear dielectric with $\varepsilon = \varepsilon_{e2}$ ($l + l_1 + d_1 < z < l + l_1 + d_1 + d_2$) followed by the other ideal metal ($z > l + l_1 + d_1 + d_2$). The solutions for the potential in the four non-metal regions between $z = 0$ and $z = l + l_1 + d_1 + d_2$ are convenient to write down in the form

$$\varphi_{d1k} = C_1 \sinh kz, \quad (9)$$

$$\varphi_{fk} = E \sin q(z - d_1) + D \cos q(z - d_1), \quad (10)$$

$$\varphi_{pk} = G \sinh k(z - l - d_1) + F \cosh k(z - l - d_1), \quad (11)$$

$$\varphi_{d2k} = C_2 \sinh k(z - l - l_1 - d_1) + B \cosh k(z - l - l_1 - d_1). \quad (12)$$

The presence of the ideal metal at $z < 0$ is taken into account in Eq. (9) via assigning zero potential. The convenience of choice of other arguments will be seen below.

From the conditions at the interface between the first dead layer and the ferroelectric at $z = d_1$, i.e., between the real metal and the ferroelectric, we have

$$C_1 \sinh kd_1 = D, \quad (13)$$

$$C_1 \varepsilon_{e1} \cosh kd_1 = -|\varepsilon_k| q E, \quad (14)$$

or

$$E = -C_1 \frac{\varepsilon_{e1}}{\sqrt{\varepsilon_{\perp} |\varepsilon_k|}} \cosh kd_1. \quad (15)$$

From the boundary conditions at the interface between the ferroelectric and the paraelectric ($z = l + d_1$), we have

$$E \sin ql + D \cos ql = F, \quad (16)$$

or

$$F = C_1 \cosh kd_1 \cos ql \left(\tanh kd_1 - \frac{\varepsilon_{e1}}{\varepsilon_p \zeta} \tan ql \right), \quad (17)$$

where

$$\zeta = \frac{\sqrt{\varepsilon_{\perp} |\varepsilon_k|}}{\varepsilon_p}, \quad (18)$$

and

$$-|\varepsilon_k| q (E \cos ql - D \sin ql) = \varepsilon_p k G, \quad (19)$$

or

$$G = C_1 \cosh kd_1 \cos ql \left(\frac{\varepsilon_{e1}}{\varepsilon_p} + \zeta \tan ql \tanh kd_1 \right), \quad (20)$$

and using the condition at the interface between the paraelectric and the second dead layer ($z = l + l_1 + d_1$) we have

$$G \sinh kl_1 + F \cosh kl_1 = B, \quad (21)$$

or

$$B = C_1 \cosh kd_1 \cos ql \cosh kl_1 \left[\left(\frac{\varepsilon_{e1}}{\varepsilon_p} + \zeta \tan ql \tanh kd_1 \right) \tanh kl_1 + \tanh kd_1 - \frac{\varepsilon_{e1}}{\varepsilon_p \zeta} \tan ql \right], \quad (22)$$

and

$$\varepsilon_p (G \cosh kl_1 + F \sinh kl_1) = \varepsilon_{e2} C_2, \quad (23)$$

or

$$C_2 = \frac{\varepsilon_p}{\varepsilon_{e2}} C_1 \cosh kd_1 \cos ql \cosh kl_1 \left[\left(\tanh kd_1 - \frac{\varepsilon_{e1}}{\varepsilon_p \zeta} \tan ql \right) \tanh kl_1 + \frac{\varepsilon_{e1}}{\varepsilon_p} + \zeta \tan ql \tanh kd_1 \right]. \quad (24)$$

Finally, at the interface between the second dead layer and the ideal metal, we have

$$C_2 \sinh kd_2 + B \cosh kd_2 = 0, \quad (25)$$

which, after substitution of Eqs. (19) and (21), converts into

$$\begin{aligned} \tan ql \left(-\frac{1}{\varepsilon_p \zeta} - \frac{1}{\zeta} \tanh kl_1 \frac{\tanh kd_2}{\varepsilon_{e2}} + \zeta \tanh kl_1 \frac{\tanh kd_1}{\varepsilon_{e1}} \right. \\ \left. + \varepsilon_p \zeta \frac{\tanh kd_1 \tanh kd_2}{\varepsilon_{e1} \varepsilon_{e2}} \right) + \frac{1}{\varepsilon_p} \tanh kl_1 + \frac{\tanh kd_1}{\varepsilon_{e1}} + \frac{\tanh kd_2}{\varepsilon_{e2}} \\ + \varepsilon_p \tanh kl_1 \frac{\tanh kd_1 \tanh kd_2}{\varepsilon_{e1} \varepsilon_{e2}} = 0. \end{aligned} \quad (26)$$

This is the condition of existence of nontrivial solutions for a given k of transcendental equation for $|\varepsilon_k|(k) = |\varepsilon_{ks}|(k)$ at the point of loss of stability of the paraelectric phase with respect to a ‘‘polarization wave’’ with a given k . In what follows, we considered the case of identical electrodes only ($d_1 = d_2 = d$, $\varepsilon_{e1} = \varepsilon_{e2} = \varepsilon_e$). This equation is solved numerically with constants for BaTiO₃ taken from Ref. 31, and ε_b and g from Ref. 34, while the parameters of the electrodes (d and ε_e) are discussed in Sec. V. Using then Eq. (6), we find $A_s(k)$ which is the value of A corresponding to the loss of stability of paraelectric phase with respect to a ‘‘polarization wave’’ $P_z(x, z) = P_{zk}(z) \cos kx$. The function $P_{zk}(z)$ is calculated from the corresponding ‘‘potential wave’’ with the help of Eq. (4), while the potential wave is given by Eq. (10) where, after solving the system of Eqs. (13)–(25) (possible if Eq. (26) is fulfilled), only one of the constants E, D remains undefined. This constant plays the role of ‘‘amplitude’’ of the polarization wave with respect to which the stability is lost for a given k . This amplitude is not defined in a stability loss analysis. The next step is to find maximum of function $A_s(k)$, which we denote as $k = k_c$. The value $A_s(k_c)$ defines the real temperature of the stability loss and it is what we present in the plots. A small but important part of the calculations can be performed analytically. Although it refers to nonphysical regions of both thicknesses and temperatures, the results can be used to check the validity of the numerics and for qualitative explanation of some results for the physical regions. Specifically, in the limit $l \rightarrow 0$, the loss of stability of PE phase is always with respect to appearance of the SD state. This has been shown first in Ref. 28 and then confirmed by several authors for different systems. The physical reason is that diminishing of the depolarizing field due to domain formation is most effective when the domain width is much less than the layer thickness and is ineffective in the opposite limit. A formal mathematical proof for the systems studied in this work can be found in supplementary material Sec. 2.³⁵ Since the coefficient B in Eq. (1) is positive, this means that in this limit there is a PE-SD phase transition of second order. The temperature of this transition is easy to calculate. It is sufficient to consider the limit $k = 0$ in Eq. (26). This corresponds to the loss of stability of PE phase with respect to formation of SD state. One finds

$$|\varepsilon| = l/\tilde{l}_{11}, \quad (27)$$

where

$$\tilde{l}_{11} = \frac{l_1}{\varepsilon_p} + \frac{d_1}{\varepsilon_{e1}} + \frac{d_2}{\varepsilon_{e2}}, \quad (28)$$

or, using Eq. (6)

$$A_{s1}(k=0) = -\varepsilon_0^{-1} \tilde{l}_{11} (l + \varepsilon_b \tilde{l}_{11})^{-1}. \quad (29)$$

$$\begin{aligned} & \frac{2}{\varepsilon_p \zeta} (\zeta \tanh kl_1 - \tan ql) \left(1 + \tan ql \tanh kl_1 \frac{\zeta^2 - 1}{2\zeta} \right) + \frac{\tanh kd_1}{\varepsilon_{e1}} \left(1 - \tan^2 ql + \tanh^2 kl_1 + \frac{3\zeta^2 - 1}{\zeta} \tan ql \tanh kl_1 + \zeta^2 \tan^2 ql \tanh^2 kl_1 \right) \\ & + \frac{\tanh kd_2}{\varepsilon_{e2}} \left(1 - \tan^2 ql + \tanh^2 kl_1 + \frac{\zeta^2 - 3}{\zeta} \tan ql \tanh kl_1 + \frac{\tan^2 ql \tanh^2 kl_1}{\zeta^2} \right). \\ & = -\varepsilon_p \frac{\tanh kd_1 \tanh kd_2}{\varepsilon_{e1} \varepsilon_{e2}} \left(2 \tanh kl_1 + 2\zeta \tan ql + (\zeta^2 - 1) \tan^2 ql \tanh kl_1 + \frac{\zeta^2 - 1}{\zeta} \tan ql \tanh^2 kl_1 \right). \end{aligned} \quad (31)$$

The rest of the procedure is the same as for the case of 1BL. For the limit $k=0$, we have now

$$|\varepsilon| = l/\tilde{l}_{12}, \quad (32)$$

where

$$\tilde{l}_{12} = \frac{l_1}{\varepsilon_p} + \frac{d_1}{2\varepsilon_{e1}} + \frac{d_2}{2\varepsilon_{e2}}, \quad (33)$$

or, using Eq. (6)

$$A_{s2}(k=0) = -\varepsilon_0^{-1} \tilde{l}_{12} (l + \varepsilon_b \tilde{l}_{12})^{-1}. \quad (34)$$

At $l \rightarrow 0$ with fixed ratio of thicknesses of FE and PE layers (l/l_1), Eq. (30) gives the same value of A for the stability loss as Eq. (34)

$$A_{s2}(k=0, l \rightarrow 0) = A_{s1}(k=0, l \rightarrow 0) = \varepsilon_0^{-1} \varepsilon_b^{-1}. \quad (35)$$

This is in a strong contrast with the case of ideal electrodes ($d_1 = d_2 = 0$) obtainable from the same formulas

$$A_{s2}^{ideal}(k=0, l \rightarrow 0) = A_{s1}^{ideal}(k=0, l \rightarrow 0) = \varepsilon_0^{-1} \varepsilon_p^{-1}. \quad (36)$$

Since $\varepsilon_p \gg \varepsilon_b$, the temperature for the transition corresponding to Eq. (36) is much higher than that corresponding to Eq. (35). This observation is important for interpretation of differences between the phase diagrams for ideal and non-ideal cases (see below).

IV. LIMIT OF STABILITY OF SINGLE-DOMAIN FERROELECTRIC STATE

As mentioned in Sec. II, to study stability of the SD state we have to linearize Eq. (2) near the value of spontaneous polarization (P_{zs}) in this state. Putting $P_z = P_{zs} + P'_z$, $E_z = E_{zs} + E'_z$,

At $l \rightarrow 0$ and with fixed ratio of thicknesses of FE and PE layers (l/l_1), we find that if stability loss of PE state is with respect to SD state it is given by the condition

$$A_{s1}(k=0, l \rightarrow 0) = \varepsilon_0^{-1} \varepsilon_b^{-1}. \quad (30)$$

For two bilayers with two real electrodes, the calculations are similar but more lengthy. Instead of Eq. (26), we obtain

substituting into Eq. (2), and omitting nonlinear in P'_z terms, we obtain

$$(A + 3BP_{zs}^2)P'_z - g \frac{\partial^2 P'_z}{\partial x^2} = E'_z, \quad (37)$$

given that

$$AP_{zs} + BP_{zs}^3 = E_{zs}, \quad (38)$$

since the SD state is homogeneous as we suppose interfaces neither promoting nor hampering ferroelectricity. Calculation of P_{zs} and E_{zs} , the depolarizing field in SD state in multilayers with homogeneous polarizations of the ferroelectric and paraelectric, was done by many authors and it is quite straightforward to take into account the presence of the real electrodes (the dead layers). Consider a system of N bilayers with real electrodes. Since the electric displacement vector, \mathbf{D} , is constant along the dielectric part of the system, we have from $\text{div } \mathbf{D} = 0$

$$\varepsilon_{e1} E_{d1} = \varepsilon_b E_{zs} + P_{zs}/\varepsilon_0 = \varepsilon_p E_p = \varepsilon_{e2} E_{d2}, \quad (39)$$

where $E_{d1,2}$ and E_p are electric fields in the dead layers and the paraelectric, respectively. From these equations and the condition of short-circuiting

$$E_{d1} d_1 + N E_{zs} + N l_1 E_p + E_{d2} d_2 = 0, \quad (40)$$

one obtains

$$E_{zs} = -\frac{P_{zs} \tilde{l}_{1N}}{\varepsilon_0 (l + \varepsilon_b \tilde{l}_{1N})}, \quad (41)$$

where

$$\tilde{l}_{1N} = \frac{l_1}{\varepsilon_p} + \frac{d_1}{N \varepsilon_{e1}} + \frac{d_2}{N \varepsilon_{e2}}. \quad (42)$$

Substituting Eq. (41) into Eq. (38) we find

$$P_{zs}^2 = -\frac{A + \varepsilon_0^{-1} \tilde{l}_{1N} (l + \varepsilon_b \tilde{l}_{1N})^{-1}}{B}, \quad (43)$$

and substituting into Eq. (37) we obtain a homogeneous equation

$$\bar{A} P'_z - g \frac{\partial^2 P'_z}{\partial x^2} = 0, \quad (44)$$

where

$$\bar{A} = -2A - 3\tilde{l}_{1N} \varepsilon_0^{-1} (l + \varepsilon_b \tilde{l}_{1N})^{-1}. \quad (45)$$

Since Eq. (44) is analogous to Eq. (3), one has just to substitute A for \bar{A} in Eqs. (3) and (6) to find the conditions of loss of stability of the SD state with respect to perturbations with given k instead of Eqs. (26) and (31). Recall that the temperature of real loss of stability of the SD state corresponds to the minimal value of $A_s(k)$ found from these equations after substitution of A for \bar{A} and putting correspondingly $N = 1, 2$.

V. RESULTS AND DISCUSSION

The results for the stability loss curves in the temperature-thickness plane are provided in Figs. 2(a)–2(d). Every figure contains curves for the ideal electrode case (this case is presented in more detail in the supplementary material 1, see Ref. 35). By putting $d_1 = d_2 = 0$ or $\varepsilon_{e1} = \varepsilon_{e2} = \infty$ in Eqs. (26) and (31) and curves for 1 BL and 2 BLs with non-ideal electrodes considering one of two cases: one is with realistically non-ideal electrodes: $d_1 = d_2 = d = 1 \text{ \AA}$ and $\varepsilon_{e1} = \varepsilon_{e2} = \varepsilon_e = 10$ so that d/ε_e is close to that of reported for SrRuO₃ in Ref. 36 and of “almost ideal” electrodes with $d = 1 \text{ \AA}$ and $\varepsilon_e = 100$. In the rest of the text, we

call “realistically non-ideal electrodes” as “non-ideal” and the other case as “almost ideal.” Both cases are studied for two ratios of thicknesses of ferroelectric and paraelectric layers FE/PE = $l/l_1 = 1/1$ (Figs. 2(a) and 2(b)) and FE/PE = $5/1$ (Figs. 2(c) and 2(d)). The interval of experimentally studied ratios FE/PE is very broad from 1/30 in Ref. 6 to 10 in Ref. 15, but since our aim is to reveal mainly qualitative and semi-quantitative tendencies we restrict ourselves by the two above options. The more that to demonstrate our main qualitative result we need not to consider small values of the ratio, see below. The lines of the stability loss for the PE phase are designated as PE/MD which means the loss of stability of PE phase with respect to formation of MD state. Similarly, SD/MD line denotes the loss of stability of SD state with respect to formation of MD state. Note that while the PE/MD line is a boundary of thermodynamic stability of both of PE and MD states, a similar statement is not correct about SD/MD line. The matter is that while the phase transition between PE and MD states is continuous (second order), the transition between SD and MD states is discontinuous.²⁹ Thermodynamically, such phase transitions occur when both phases are stable and their energies are equal. Loss of stability of SD state which we consider occurs at a higher temperature (the limit of the overheating), i.e., the region of thermodynamical instability of the SD phase is broader than according to our calculations.

We provide results for temperatures down to $-273 \text{ }^\circ\text{C}$, i.e., to almost absolute zero and for thicknesses of the ferroelectric layer (l) beginning with zero, i.e., we include subatomic thicknesses though in a very small part of l -axis. This is made for convenience of presentation of the results of the continuum medium theory: the case for $l \rightarrow 0$ is possible to treat analytically as it was shown above. Broader range of temperatures including the non-physical ones is presented in supplementary material 3 once again for a better comprehension of

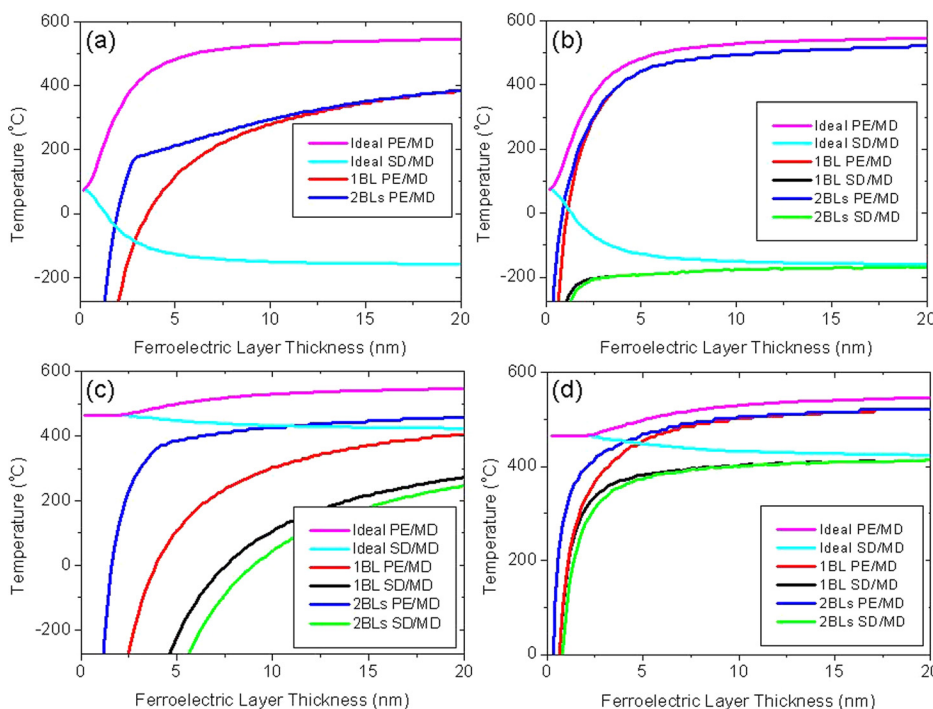


FIG. 2. The PE/MD and SD/MD stability limit curves for (a) FE/PE = 1/1 system with $d_1 = d_2 = 1 \text{ \AA}$ and $\varepsilon_{e1} = \varepsilon_{e2} = 10$, (b) FE/PE = 1/1 system with $d_1 = d_2 = 1 \text{ \AA}$ and $\varepsilon_{e1} = \varepsilon_{e2} = 100$, (c) FE/PE = 5/1 system with $d_1 = d_2 = 1 \text{ \AA}$ and $\varepsilon_{e1} = \varepsilon_{e2} = 10$, and (d) FE/PE = 5/1 system with $d_1 = d_2 = 1 \text{ \AA}$ and $\varepsilon_{e1} = \varepsilon_{e2} = 100$. The data for the ideal electrodes are given in all plots for comparison.

the mathematical results. In all Figs. 2(a)–2(d), the curves for systems with non-ideal electrodes are below the curves for ideal electrodes which could be, of course, anticipated. What is, however, unexpected are magnitudes of some shifts together with their dependence on BL number, i.e., the difference between 1BL and 2BL cases.

Beginning with FE/PE = 1/1 (Figs. 2(a) and 2(b)) we see SD/MD curves, while in the unphysical region in the non-ideal electrode case, they are in the physical region for “almost ideal” electrodes. However, it is not certain whether the SD state is thermodynamically stable or metastable in the range shown in Fig. 2(b) for the reasons discussed above. Remarkable here is the lowering of temperature of phase transition from the PE state for “realistically non-ideal electrodes”: it is 200 to 300 °C for $l > 3\text{--}4$ nm and even a more rapid fall of the phase transition temperature for smaller thicknesses. For $l < 1.5$ nm (Fig. 2(a)), there is no phase transition from the paraelectric phase in the system. The precise numerical values are not of much importance here. In fact, these results seemingly contradict to experimental data of Ref. 37 where ferroelectric phase transition at $T = 70$ K has been observed in 1.6 nm BaTiO₃ film on dielectric SrTiO₃ substrate and without top electrode (but in air). The phase transition temperature in such a system is naturally expected to be lower than according to our results, whilst just the opposite is observed. However, there are several possible reasons of such disagreement beginning from our use of temperature-independent values for ϵ_{\perp} and ϵ_p , while at low temperatures they are several times higher than what we used as it was discussed above. This shortcoming is relatively easy to remedy unlike the uncertainty in numerical value of the constant g that was commented on in Ref. 34 where we have retrieved this constant from. The real information reported by Fig. 2(a) is that influence of non-ideality of the electrodes is quite strong, especially for small thicknesses and that the temperature of the phase transition is higher for 2BL systems than for 1BL ones. If this tendency remains at further increase of the BL number one might, probably, expect that the PE/MD curve for superlattices with high number of repeating units is fairly close to the case of ideal electrodes.

An opposite situation occurs for the SD/MD curves (for non-ideal electrodes) which are beyond the physical region of the FE/PE = 1/1 (Fig. 2(a)) but are partially within physical T - l regime for FE/PE = 5/1 (Fig. 2(c)). The qualitative character of the phase diagram is the same both for 1/1 and 5/1 cases which is seen when the non-physical region is also presented (see supplementary material 3 (Ref. 35)) so that it is sufficient to comment on the 5/1 case. One sees that the SD/MD curve for 2BL system is below the 1BL one. If this tendency remains at further increase of the BL number, one should consider our results for region of absolute instability of SD state as the lower limit for this region, i.e., for superlattices with large number of BLs the region of absolute instability of SD state should be wider. Note that the behavior of the SD/MD curve is qualitatively different for ideal and non-ideal electrodes: the curve goes from upper left to lower right in the ideal case, but from lower left to upper right for non-ideal electrodes. The reason is the dramatic

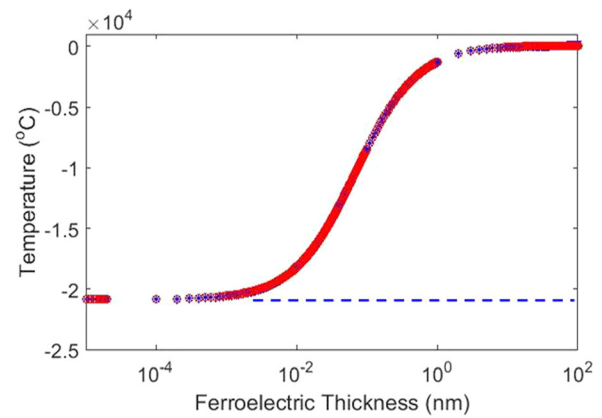


FIG. 3. PE/MD and SD/MD stability limit curves including the unphysical temperature/thickness regime. Please note that due to the strong overlap, it is difficult to distinguish the curves, especially below 1 nm FE thickness. Black data are for the PE/MD and the red data are for the SD/MD. The dashed blue line indicates the analytical solution of $-21\,400$ °C.

difference in position the $l = 0$ point in the two cases (compare Eqs. (35) and (36)). In the non-ideal case, this point is very far in the non-physical region: approx. $-21\,400$ °C for the material constants which we use, and this is practically the beginning for the SD/MD curve which is in non-physical region not only for temperature but also, of course, for thicknesses which is much smaller than the unit cell distance. The curve climbs up already in the region of unphysical thicknesses (see Fig. 3) but this still corresponds to unphysical temperatures all the way until around several unitcell thickness after which it continues to go up with increasing of thickness of the FE layer. It is clear that physically, the more the thickness the easier for the ferroelectric to diminish the depolarizing field due to formation of the domain structure so that in the limit of large l the behavior of systems with non-ideal and ideal electrodes is similar.

Note that due to the non-ideality of the electrodes, a dramatic decrease of region occurs where the SD state is either stable or metastable. Only in Fig. 2(d), i.e., for FE/PE = 5/1 and “almost ideal” electrode situation, this region is completely within physically meaningful intervals of T and l . Recalling that for $l \rightarrow 0$, the phase transition from paraelectric phase is (formally) always into a single domain state; let us also compare the thicknesses until which this statement remains valid (formally, of course, since we also include now the subatomic thicknesses) in the cases of ideal and non-ideal electrodes. One sees from Fig. S1 of the supplementary material³⁵ that in the case of ideal electrodes, this thickness is about 0,4 nm if FE/PE = 1/1 nm, while for the same FE/PE ratio but for “non-ideal electrode” it is profoundly in the non-physical region, see Fig. 3. The exact value of $-21\,400$ °C for the “phase transition into SD state” at $l \rightarrow 0$ has been obtained from Eq. (35) and the limit when $l \rightarrow 0$ in the curve is obtained from numerical solution of Eq. (26) (see the horizontal line in the unphysical regime approx. $-21\,000$ °C in Fig. 3), which also served us as an excellent test of the correctness of the numerical procedure and precision.

Two considered variants of the FE/PE volume fraction seem to give sufficient qualitative information about absolute

instability of SD state. The choice of 1/1 option hardly needs justification. This is a natural starting point. We see that the SD/MD curve for this option is well beyond the physical region for the used material constants. Naturally, one would want to have the SD/MD curve inside the physical region because it is of practical interest for applications. To this aim, we increase the volume fraction of the ferroelectric material, i.e., go to the 5/1 case and achieve our goal, at least partially. We have no motivation to check with volume fractions corresponding to $FE/PE < 1$ because it would shift the SD/MD curve even further into the non-physical region. Recall that increase in the BL number shifts the SD/MD curve to even lower temperatures if the tendency revealed when comparing 1BL and 2BL cases persists for higher numbers of the repeating units.

VI. CONCLUSIONS

The main message of this paper is that influence of non-ideality of the electrodes on properties of ferroelectric-paraelectric superstructures is unexpectedly strong. As a result of this influence, it could be problematic to obtain single-domain states in the superstructures and special conditions seem necessary to achieve this goal. In addition, it is very challenging to treat the superlattices with non-ideal electrodes and in multi-domain states analytically since this involves quite a lengthy algebra which becomes tedious the more is the number of repeating units in the considered superstructure. That is why we were forced to limit ourselves by systems with one and two ferroelectric-paraelectric bilayers speculating that the differences in properties of the systems give us a qualitative insight into properties of superlattices with many repeating units. It is highly desirable, of course, to explicitly confirm the guesses. Only electrostatic effects have been taken into account and no specific properties of different interfaces: between the layers and between the electrodes and the material. This is, once more, because of technical complexity of the problem as well as lack of reliable information about the interfaces.

ACKNOWLEDGMENTS

A.P.L. was partially supported by Russian Foundation of Basic Research Grant No. 13-02-12459-ofi-m.

- ¹K. Iijima, T. Terashima, Y. Bando, K. Kamigaki, and H. Terauchi, *J. Appl. Phys.* **72**, 2840 (1992).
- ²H. Tabata, H. Tanaka, and T. Kawai, *Appl. Phys. Lett.* **65**, 1970 (1994).
- ³E. D. Specht, H. M. Christen, D. P. Norton, and L. A. Boatner, *Phys. Rev. Lett.* **80**, 4317 (1998).
- ⁴H. M. Christen, E. D. Specht, D. P. Norton, M. F. Chisholm, and L. A. Boatner, *Appl. Phys. Lett.* **72**, 2535 (1998).
- ⁵A. L. Roytburd, S. Zhong, and S. P. Alpay, *Appl. Phys. Lett.* **87**, 092902 (2005).
- ⁶V. A. Stephanovich, I. A. Luk'yanchuk, and M. G. Karkut, *Phys. Rev. Lett.* **94**, 047601 (2005).

- ⁷H. N. Lee, H. M. Christen, M. F. Chisholm, C. M. Rouleau, and D. H. Lowndes, *Nature* **433**, 395 (2005).
- ⁸W. Tian, J. C. Jiang, X. Q. Pan, J. H. Haeni, Y. L. Li, L. Q. Chen, D. G. Schlom, J. B. Neaton, K. M. Rabe, and Q. X. Jia, *Appl. Phys. Lett.* **89**, 092905 (2006).
- ⁹D. A. Tenne, A. Bruchhausen, N. D. Lanzillotti-Kimura, A. Fainstein, R. S. Katiyar, A. Cantarero, A. Soukiassian, V. Vaithyanathan, J. H. Haeni, W. Tian, D. G. Schlom, K. J. Choi, D. M. Kim, C. B. Eom, H. P. Sun, X. Q. Pan, Y. L. Li, L. Q. Chen, Q. X. Jia, S. M. Nakhmanson, K. M. Rabe, and X. X. Xi, *Science* **313**, 1614 (2006).
- ¹⁰Y. L. Li, S. Y. Hu, D. Tenne, A. Soukiassian, D. G. Schlom, X. X. Xi, K. J. Choi, C. B. Eom, A. Saxena, T. Lookman, Q. X. Jia, and L. Q. Chen, *Appl. Phys. Lett.* **91**, 112914 (2007).
- ¹¹D. G. Schlom, L. Q. Chen, C. B. Eom, K. M. Rabe, S. K. Streiffer, and J. M. Triscone, *Annu. Rev. Mater. Res.* **37**, 589 (2007).
- ¹²A. Soukiassian, W. Tian, V. Vaithyanathan, J. H. Haeni, L. Q. Chen, X. X. Xi, D. G. Schlom, D. A. Tenne, H. P. Sun, X. Q. Pan, K. J. Choi, C. B. Eom, Y. L. Li, Q. X. Jia, C. Constantin, R. M. Feenstra, M. Bernhagen, P. Reiche, and R. Uecker, *J. Mater. Res.* **23**, 1417 (2008).
- ¹³V. R. Cooper and K. M. Rabe, *Phys. Rev. B* **79**, 180101 (2009).
- ¹⁴J. Hlinka, V. Zelezny, S. M. Nakhmanson, A. Soukiassian, X. X. Xi, and D. G. Schlom, *Phys. Rev. B* **82**, 224102 (2010).
- ¹⁵P. Zubko, N. Stucki, C. Lichtensteiger, and J. M. Triscone, *Phys. Rev. Lett.* **104**, 187601 (2010).
- ¹⁶A. P. Levanyuk and I. B. Misirlioglu, *J. Appl. Phys.* **110**, 114109 (2011).
- ¹⁷A. Torres-Pardo, A. Gloter, P. Zubko, N. Jecklin, C. Lichtensteiger, C. Colliex, J. M. Triscone, and O. Stephan, *Phys. Rev. B* **84**, 220102 (2011).
- ¹⁸K. Kathan-Galipeau, P. P. Wu, Y. L. Li, L. Q. Chen, A. Soukiassian, X. X. Xi, D. G. Schlom, and D. A. Bonnell, *ACS Nano* **5**, 640 (2011).
- ¹⁹P. Zubko, N. Jecklin, A. Torres-Pardo, P. Aguado-Puente, A. Gloter, C. Lichtensteiger, J. Junquera, O. Stephan, and J. M. Triscone, *Nano Lett.* **12**(6), 2846–2851 (2012).
- ²⁰P. Chen, J. Y. Jo, H. N. Lee, E. M. Dufresne, S. M. Nakhmanson, and P. G. Evans, *New J. Phys.* **14**, 013034 (2012).
- ²¹P. Aguado-Puente and J. Junquera, *Phys. Rev. B* **85**, 184105 (2012).
- ²²Y. F. Duan, G. Tang, C. Q. Chen, T. J. Lu, and Z. G. Wu, *Phys. Rev. B* **85**, 054108 (2012).
- ²³A. P. Levanyuk and I. B. Misirlioglu, *Appl. Phys. Lett.* **103**, 192906 (2013).
- ²⁴P. Chen, M. P. Cosgriff, Q. T. Zhang, S. J. Callori, B. W. Adams, E. M. Dufresne, M. Dawber, and P. G. Evans, *Phys. Rev. Lett.* **110**, 047601 (2013).
- ²⁵N. Ortega, A. Kumar, O. Resto, O. A. Maslova, Y. I. Yuzyuk, J. F. Scott, and R. S. Katiyar, *J. Appl. Phys.* **114**, 104102 (2013).
- ²⁶I. B. Misirlioglu, M. T. Kesim, and S. P. Alpay, *Appl. Phys. Lett.* **104**, 022906 (2014).
- ²⁷I. B. Misirlioglu, M. T. Kesim, and S. P. Alpay, *Appl. Phys. Lett.* **105**, 172905 (2014).
- ²⁸E. V. Chensky and V. V. Tarasenko, *Sov. Phys. - JETP* **56**, 618 (1982); *Zh. Eksp. Teor. Fiz.* **83**, 1089 (1982).
- ²⁹A. M. Bratkovsky and A. P. Levanyuk, *J. Comput. Theor. Nanosci.* **6**, 465 (2009).
- ³⁰D. R. Tilley and J. Tilley, *Superconductivity and Superfluidity* (Van Nostrand Reinhold, London, 1974).
- ³¹N. A. Pertsev, A. G. Zembilgotov, and A. K. Tagantsev, *Phys. Rev. Lett.* **80**, 1988 (1998).
- ³²A. Onodera, Y. Kawamura, T. Okabe, and H. Terauchi, *J. Eur. Ceram. Soc.* **19**, 1477 (1999).
- ³³A. K. Tagantsev, *Ferroelectrics* **375**, 19 (2008); A. K. Tagantsev and G. Gerra, *J. Appl. Phys.* **100**, 051607 (2006).
- ³⁴J. Hlinka and P. Marton, *Phys. Rev. B* **74**, 104104 (2006).
- ³⁵See supplementary material at <http://dx.doi.org/10.1063/1.4939779> for the ideal electrode results, SD stability in the ultrathin thickness limit of the ferroelectric, and stability curves in the extended parameter regime.
- ³⁶G. Gerra, A. K. Tagantsev, and N. Setter, *Phys. Rev. Lett.* **98**, 207601 (2007).
- ³⁷D. A. Tenne *et al.*, *Phys. Rev. Lett.* **103**, 177601 (2009).